Romanian Reports in Physics **73**, 112 (2021)

MATHEMATICAL AND NUMERICAL INVESTIGATIONS OF THE FRACTIONAL-ORDER EPIDEMIC MODEL WITH CONSTANT VACCINATION STRATEGY

ZAFAR IQBAL[1], MUHAMMAD AZIZ UR REHMAN[1], DUMITRU BALEANU[2,3,4,*], NAUMAN AHMED[5], ALI RAZA[6], MUHAMMAD RAFIQ[7]

[1]Department of Mathematics, University of Management and Technology, Lahore, Pakistan
Email: *zafariqbal0092@gmail.com; aziz.rehman@umt.edu.pk*
[2]Department of Mathematics, Cankaya University, 06530, Balgat, Ankara, Turkey
[*]Corresponding author, Email: *dumitru.baleanu@gmail.com*
[3]Department of Medical Research, China Medical University Hospital, China Medical University, Taichung, Taiwan
[4]Institute of Space Sciences, Magurele-Bucharest, Romania
[5]Department of Mathematics and Statistics, The University of Lahore, Lahore, Pakistan
Email: *nauman.ahmd01@gmail.com*
[6]Department of Mathematics, National College of Business Administration and Economics Lahore, Pakistan
Email: *alimustasamcheema@gmail.com*
[7]Department of Mathematics, Faculty of Sciences, University of Central Punjab, Lahore, Pakistan
Email: *m.rafiq@ucp.edu.pk*

Received November 19, 2020

Abstract. This work is devoted to find the reliable numerical solution of an epidemic model with constant vaccination strategy. For this purpose, a structure preserving numerical scheme called the Grünwald-Letnikov nonstandard finite difference scheme is designed. The proposed technique retains all the important properties of the continuous epidemic model like boundedness, positivity, and stability. This behavior of the proposed numerical scheme is validated mathematically and graphically. The role of the vaccination in controlling the disease dynamics in the population is verified through numerical simulations. The stability of the system under discussion is also examined at the disease free equilibrium point and the endemic equilibrium point. Finally, the outcome of this study is furnished with concluding remarks and future directions of research.

Key words: Grünwald-Letnikov nonstandard method, fractional-order epidemic model, constant vaccination strategy, numerical methods.

1. INTRODUCTION

Many infectious diseases are fatal to the mankind. These diseases resulted in economic loss and public health deterioration [1]. Some of them can be controlled at the early stage, also known as acute stage. There are some diseases that can be eradicated only by vaccinating the children under certain age, for instance Polio. The

antibiotics and certain other medicines are also serving the community by controlling the infections. Some diseases can be avoided by following the precautionary measures. The use of vaccine gained the remarkable attention during the recent past as they have eliminated, even eradicated a number of infectious diseases [2]. Despite these facts, some fatal infectious diseases are continuously invading the different communities around the globe. With the development of bio-medicines and life sciences, new infectious diseases are also arising. So, it is a permanent challenge to health caretakers and policy makers.

Cholera, malaria, influenza, hemorrhagic fever, and tuberculosis are still responsible for most of the diseases and mortalities in the world [3]. It is the mode of disease transmission that helps a lot to understand the epidemiology in a comprehensive way. Different diseases have different routes of transmission, some of them have multiple routes, however all the routes are not well elaborated. Some authors focussed on the dominant route for disease transmission and addressed some effective and efficient disease control strategies [4]. The disease transmission mode may be vertical as well as horizontal. Vertical mode occurs through vaginal birth, transplacental or breast feeding. While the horizontal transmission involves sexual (*i.e.* through flower to flower, or oro-genital) transmission. Non sexual transmission may take place through direct contact, airborne or indirectly. Mainly, the indirect transmission occurs by environment (*i.e.* contaminated food, water etc.), fomites and vectors [5].

Direct or indirect contact of the host plays a vital role in disease transmission [6]. Direct contact transmission means physical contact and transfer of the infection is occurred through the infected person. On the other hand the indirect contact transmission takes place through pathogens or fomites. Infectious aerosols also make the direct contact transmission that travel short distance from the source and make the disease spread in the susceptible individuals [7]. Also, the indirect contact transmission takes place through skin flakes, fungal spores, and aerosol that travel longer distance to transport pathogens [8]. One of the effective control strategies in preventing the disease is hindering the main route of the disease transmission. Quarantine of the infected persons is also a basic and important technique to prevent the further transmission of the infection. The wearing of the mask against respiratory like pneumonia and COVID-19 diseases and use of the disinfectants to kill the pathogen could effectively control the disease communication [9]. Some traditional practices also provide a foundation to prevent and control the infection. These practices involve the use of personal protective equipments. The most important precautionary measure against some diseases is the hand hygiene all the time. Focussing on the nature and severeness of the infection, many researchers constructed the various disease models to discuss the mechanism of the disease, see, for example, Refs. [10–20]. Some well known compartmental models are SI, SIR, SIRS, and SEIQV. By studying the

literature, SIR model seems to be the favorite model of many researchers because of its simplicity. Furthermore, these models are easy to understand and apply.

In recent years, fractional calculus has been used to study a plethora of relevant linear and nonlinear models arising in mathematics, physics, technical sciences, and biophysics, see, for example, some recent works in this broad research area [21–33].

In this work, we consider a fractional SIR epidemic model with constant vaccination strategy, where the population is divided into three compartments, *i.e.* susceptible $\mathcal{S}(t)$, infected $\mathcal{I}(t)$, and recovered $\mathcal{R}(t)$. The SIR fractional-order compartmental epidemic model is represented analytically by the following nonlinear system

$$
\begin{aligned}
{}_0^{\mathcal{C}}D_t^{\alpha}\mathcal{S}(t) &= (1-P)\mu^{\alpha} - \beta^{\alpha}\mathcal{S}(t)\mathcal{I}(t) - \mu^{\alpha}\mathcal{S}(t) && (1)\\
{}_0^{\mathcal{C}}D_t^{\alpha}\mathcal{I}(t) &= \beta^{\alpha}\mathcal{S}(t)\mathcal{I}(t) - (\eta^{\alpha}+\mu^{\alpha})\mathcal{I}(t) && (2)\\
{}_0^{\mathcal{C}}D_t^{\alpha}\mathcal{R}(t) &= P\mu^{\alpha} + \eta^{\alpha}\mathcal{I}(t) - \mu^{\alpha}\mathcal{R}(t) && (3)
\end{aligned}
$$

where, ${}_0^{\mathcal{C}}D_t^{\alpha}$ denotes the Caputo fractional derivative operator of order α, which is defined in [14] as

$$
{}_0^{\mathcal{C}}D_t^{\alpha}u(t) = \begin{cases} \frac{1}{\Gamma(n-\alpha)}\int_0^t \frac{u^n(s)}{(t-s)^{\alpha+1-n}d}ds; & n-1 \le \alpha < n \\ \frac{d^n u(t)}{dt^n}, & \alpha = n \end{cases} \tag{4}
$$

where $0 < \alpha < 1$. The parameters of the model (1)-(3) are as follows: η^{α} is the analogous to the recovery rate from the infection, μ^{α} is the analogous to the the birth (death) rate, and the parameter β^{α} is the analogous to the beta transmission contact rate.

2. BASIC PROPERTIES OF MODEL

The fractional form of generalized mean value theorem is given below, which is one of the fundamental results as presented in [16].

Lemma 1. *If the function $g(t) \in C[a,b]$ and ${}_0^{\mathcal{C}}D_t^{\alpha}g(t) \in C(a,b]$, for $0 < \alpha \le 1$, then we have*

$$
g(t) = g(a) + {}_0^{\mathcal{C}}D_t^{\alpha}g(\xi)\frac{(t-\alpha)^{\alpha}}{\gamma(\alpha)}, \qquad 0 \le \xi \le t. \tag{5}
$$

So, if $g(t) \in C[0,b]$ and ${}_0^{\mathcal{C}}D_t^{\alpha}g(t) \in C(0,b]$ and if ${}_0^{\mathcal{C}}D_t^{\alpha}g(t) \ge 0$ then, the function g is not decreasing.

Lemma 2. *For any given non-negative initial conditions, there exists a unique solution $\mathcal{S}$, $\mathcal{I}$, $\mathcal{R}$ for all $t \ge 0$. Moreover, it satisfies the following inequality of boundedness:* $\lim_{t\to\infty}\sup N(t) \le 1$.

Proof. By adding equations (1), (2), and (3), we have

$$\begin{aligned} {}^{\mathcal{C}}_{0}D^{\alpha}_{t}\left(\mathcal{S}(t)+\mathcal{I}(t)+\mathcal{R}(t)\right) &= \mu^{\alpha}-\mu^{\alpha}\left(\mathcal{S}(t)+\mathcal{I}(t)+\mathcal{R}(t)\right) \quad (6)\\ {}^{\mathcal{C}}_{0}D^{\alpha}_{t}N(t) &= \mu^{\alpha}-\mu^{\alpha}N(t) \quad (7)\end{aligned}$$

It follows that

$$N(t)=N(0)e^{-\mu^{\alpha}t}+1. \quad (8)$$

Thus, the solutions exist for the given initial conditions that are eventually bounded on every finite time interval. □

Lemma 3. *The closed set*

$$\Gamma=\left(\mathcal{S}(t),\mathcal{I}(t),\mathcal{R}(t)\in\mathbb{R}^{3}_{+}:\mathcal{S}(t)+\mathcal{I}(t)+\mathcal{R}(t)=1\right)$$

is positive invariant.

Proof. From equations (7) and (8), it follows that if $t\to\infty$, the population is bounded by a positive number $N(t)=1$. Therefore, the set Γ is positive invariant. □

2.1. BASICS OF FRACTIONAL CALCULUS

Consider a continuous function $V=V(t)$, The first-order derivative of the function is defined by the following limit,

$$V'(t)=\frac{dV}{dt}=\lim_{h\to 0}\frac{V(t)-V(t-h)}{h}. \quad (9)$$

By applying this definition repeatedly, we reach at

$$V^{(m)}(t)=\frac{d^{m}V}{dt^{m}}=\lim_{h\to 0}\frac{1}{h^{m}}\sum_{s=0}^{m}(-1)^{s}\binom{m}{s}f(t-sh), \quad (10)$$

where $\binom{m}{s}$ is the well known notation of binomial coefficient. Now, consider the following relation, which is obtained by generalizing the Eqs. (9) and (10);

$$V_{h}^{(n)}(t)=\frac{1}{h^{n}}\sum_{s=0}^{n}(-1)^{s}\binom{n}{s}V(t-sh), \quad (11)$$

where m is an arbitrary integer and for $n\leq m$, we obtain the relation

$$\lim_{h\to 0}V_{h}^{(n)}(t)=V^{(n)}(t)=\frac{d^{n}V}{dt^{n}}.$$

Replacing n by $-n$ in (11), we have

$$V_{h}^{(-n)}(t)=\frac{1}{h^{-n}}\sum_{s=0}^{n}\binom{-n}{s}V(t-sh),$$

where $\binom{-n}{s} = (-1)^s \left[{n \atop s}\right]$, $n \in \mathbb{Z}^+$. For a fixed $n \in \mathbb{Z}^+$, $V_h^{(-n)}$ approaches to zero. To obtain the non-zero limit, we let that $m \to \infty$, as $h \to 0$, h may be taken as $\frac{t-a}{m}$. The limit of $V_h^{(-n)}$ is denoted as

$$\lim_{\substack{h\to 0 \\ mh=t-a}} V_h^{-n}(t) = {}_\alpha D_t^{-n} V(t) \tag{12}$$

Here ${}_\alpha D_t^{-n} V(t)$ represents the particular operations, operated upon the function $V(t)$; a and t are called terminals or lower and upper limits regarding to this particular operation. By considering $h = \frac{t-a}{m}$ or $t - mh = a$, $V(t)$ is considered to be continuous and the following relation can be satisfied for $n = 1$.

$$\lim_{\substack{h\to 0 \\ mh=t-a}} V_h^{-n}(t) = {}_\alpha D_t^{-n} V(t) = \int_0^{t-a} V(t-s)ds = \int_a^t V(\tau)d\tau. \tag{13}$$

By applying this operation n times, we obtain the following expression

$${}_\alpha D_t^{-n} V(t) = \lim_{\substack{h\to 0 \\ mh=t-a}} h^p \sum_{s=0}^{m} \left[{n \atop s}\right] V(t-sh) = \frac{1}{(p-1)!} \int_a^t (t-s)^{n-1} V(s)ds. \tag{14}$$

The above formula (14) can be represented as an n-fold ingral as follows. We integrate the relationship from a to t

$$\frac{d}{dt} {}_\alpha D_t^{-n} V(t) = \frac{1}{(n-2)!} \int_a^t (t-s)^{n-2} V(s)ds = {}_\alpha D_t^{-p+1} V(t).$$

We then obtain

$${}_\alpha D_t^{-n} V(t) = \int_a^t \left({}_\alpha D_t^{-n+1} V(t)\right) dt.$$

$${}_\alpha D_t^{-n+1} V(t) = \int_a^t \left({}_\alpha D_t^{-n+2} V(t)\right) dt.$$

In a similar way, we arrive at

$$\begin{aligned} {}_\alpha D_t^{-p} V(t) &= \int_a^t dt \int_a^t \left({}_\alpha D_t^{-p+2} V(t)\right) dt \\ &\quad \cdots \\ &\quad \cdots \\ &= \int_a^t dt \int_a^t dt \cdots \int_a^t V(t)dt \qquad \text{(n times)}. \end{aligned} \tag{15}$$

It can be observed that the derivative of an integer order m as given by (10) and the n-fold integral given by (15) for the continuous function $V(t)$ is the specific case of

the general relation

$$ {}_{\alpha}D_t^n V(t) = \lim_{\substack{h\to 0 \\ mh=t-a}} h^{-p} \sum_{s=0}^{m} (-1)^s \binom{n}{s} V(t-sh), \tag{16} $$

which describes the derivative of order n if $p = n$ and the n-fold integral for $p = -n$. This expression, ultimately leads to the generalization of the classical differentiation and integration by replacing n in (16) by any arbitrary real number or even by a complex number. We can find the Grünwald-Letnikov derivative as

$$ {}_{\alpha}D_t^n V(t) = \sum_{k-0}^{m} \frac{V^k(a)(t-a)^{-n+k}}{\Gamma(-m+m+1)} \int_a^t (t-\tau)^{m-n} V^{m+1}(\tau) d\tau, \tag{17} $$

the least possible value for n is given by $m < n < m+1$

Definition 1. Let $\alpha \in \mathbf{R}^+$, the Caputo fractional derivative having order α is defined as

$$ ({}_0^{\mathcal{C}}D_t^{\alpha} f)(t) = \frac{1}{\gamma(n-\alpha)} \int_0^t \frac{f^{(n)}(x)}{(t-x)^{1-n+\alpha} dx}, \qquad t > 0 \tag{18} $$

where $f(x) \in C^n[0,\infty[, n = [\alpha]+1$ and $f(x) \in C^n[0,\infty[$ is the continuous function in the given interval up to n^{th} derivative.

The above definition indicates that the derivative of the constant function is zero; for $\alpha \in N$ the Caputo integral operator coincides with the integer-order classical derivative. Moreover, the Caputo operator is linear, that is

$$ {}_0^{\mathcal{C}}D_t^{\alpha}(\alpha f(t) + \beta g(t) = \alpha {}_0^{\mathcal{C}}D_t^{\alpha} f(t) + \beta {}_0^{\mathcal{C}}D_t^{\alpha} g(t). \tag{19} $$

2.2. STABILITY ANALYSIS

In this Section, we will analyze the stability of the fractional epidemic model with constant vaccination strategy at both the equilibrium points, locally and globally.

2.2.1. Local Stability

We set the equation $g(t) = 0$ to find the points of equilbria, $g(t)$ is the left hand side of the system of equations (1)-(3). If all the eigenvalues λ_i of the Jacobian matrix $J = \frac{\partial g}{\partial t}$, calculated at equilibrium point satisfy $|\arg(\lambda i)| > \alpha\frac{\pi}{2}, i = 1,2$, then the equilibrium point is locally asymptotically stable. Let

$$ \mathcal{F} = (1-P)\mu^{\alpha} - \beta^{\alpha}\mathcal{S}\mathcal{I} - \mu^{\alpha}\mathcal{S} \tag{20} $$

$$ \mathcal{G} = \beta^{\alpha}\mathcal{S}\mathcal{I} - (\eta^{\alpha} + \alpha^{\alpha})\mathcal{I} \tag{21} $$

$$ \mathcal{H} = P\mu^{\alpha} + \eta\mathcal{I} - \mu^{\alpha}\mathcal{R} \tag{22} $$

The Jacobian matrix $\mathcal{J}$ is given as

$$\mathcal{J} = \begin{pmatrix} \mathcal{F}_{\mathcal{S}} & \mathcal{F}_{\mathcal{I}} & \mathcal{F}_{\mathcal{R}} \\ \mathcal{G}_{\mathcal{S}} & \mathcal{G}_{\mathcal{I}} & \mathcal{G}_{\mathcal{R}} \\ \mathcal{H}_{\mathcal{S}} & \mathcal{H}_{\mathcal{I}} & \mathcal{H}_{\mathcal{R}} \end{pmatrix}$$

After simplifying the Jacobian and the given system we have

$$\mathcal{J} = \begin{pmatrix} \beta^{\alpha}\mathcal{I} - \mu^{\alpha} & \beta^{\alpha}\mathcal{I} \\ -\beta^{\alpha}\mathcal{S} & \beta^{\alpha}\mathcal{S} - \eta^{\alpha} - \mu^{\alpha} \end{pmatrix}$$

At disease free equilibrium $E_d(1-P, 0)$, the Jacobian becomes

$$\mathcal{J}_{E_d} = \begin{pmatrix} -\mu^{\alpha} & 0 \\ \beta^{\alpha}(1-P) & \beta^{\alpha}(1-P) - \eta^{\alpha} - \mu^{\alpha} \end{pmatrix}$$

The eigenvalues of the matrix $\mathcal{J}_{E_d}$ are $\lambda_1 = -\mu^{\alpha}$ and $\lambda_2 = \beta^{\alpha}(1-P) - \eta^{\alpha} - \mu^{\alpha}$. Clearly $\lambda_1 < 0$ and the value of $\lambda_2 < 0$ because $R_0 < 1$.

The vaccination reproduction number is evaluated as

$$R_v = \frac{\beta^{\alpha}(1-P)}{\eta^{\alpha} + \mu^{\alpha}} \tag{23}$$

The DFE is locally stable if $\beta^{\alpha}(1-P) < \eta^{\alpha} + \mu^{\alpha}$, that is, $R_v < 1$. From equation (23) the critical vaccination proportion $P_c = \frac{\beta^{\alpha} - \eta^{\alpha} - \mu^{\alpha}}{\beta^{\alpha}}$ can be obtained, beyond this critical value the DFE is stable *i.e.* for $P > P_c$. The inequality $P > P_c$ describes the fact that when a large portion of the population is vaccinated, the disease can be controlled effectively. On the other hand, if $R_v > 1$, the DFE is not stable. In this situation the endemic equilibrium (EE) point exists and the disease persists in the community. The EE looks like

$$E_e = \left(\frac{1-P}{R_v}, \frac{\mu^{\beta}}{\beta^{\alpha}}(R_v) - 1 \right) \tag{24}$$

The eigenvalues $(e_{1,2})$ at EE(E_e) against the Jacobian matrix is given as

$$e_{1,2} = -\frac{\mu^{\alpha}}{2} R_v \pm \frac{1}{2}\sqrt{(\mu^{\alpha})^2 R_v^2 - 4R_v\mu^{\alpha}(\eta^{\alpha} + \mu^{\alpha})} \tag{25}$$

The EE is locally asymptotically stable, when

$$1 < R_v \leq \frac{4(\eta^{\alpha} + \mu^{\alpha})}{\mu^{\alpha}} \tag{26}$$

For R_v mentioned above the eigenvalues e_1, e_2 are complex, having real parts negative so E_e can be regarded as a spiral sink. This fact can be explained as follows. If the number of infected individuals in the beginning is low, then the number of susceptible individuals is large. When the infected individuals interact with the susceptible

individuals, the number of infected persons grows and this happens until the rate of infected persons becomes greater then the rate of susceptible persons. Consequently, there are a few susceptible individuals in the community to become infected. At this stage, the spread of disease comes to an end.

2.2.2. Global Stability

We now establish some results related to the global stability.

Theorem 4. *For given $t > 0$ and $0 < \alpha \leq 1$, the model (1)-(3) is said to be globally asymptotically stable at disease free equilibrium $E_d = (\mathcal{S}^1, \mathcal{I}^1) = (1-P, 0)$, which is contained in the region Γ if $R_v < 1$, otherwise unstable.*

Proof. Let us consider the Volterra-type Lyapunov function $u : \Gamma \to R$ defined as

$$\begin{aligned}
u &= \left(\mathcal{S} - \mathcal{S}^1 - \mathcal{S}^1 log\frac{\mathcal{S}}{\mathcal{S}^1}\right) + \mathcal{I}, \quad S, I \in \Gamma \\
{}^{c}_{0}D^{\alpha}_{t}u(t) &= \left(1 - \frac{S}{S^1}\right) {}^{c}_{0}D^{\alpha}_{t}\mathcal{S}(t) + {}^{c}_{0}D^{\alpha}_{t}I(t) \\
&= \left(1 - \frac{S}{S^1}\right)[(1-P)\mu^{\alpha} - \beta^{\alpha}\mathcal{S}\mathcal{I} - \mu^{\alpha}\mathcal{S}] + \beta^{\alpha}\mathcal{S}\mathcal{I} - (\eta^{\alpha} + \mu^{\alpha})\mathcal{I} \\
&= -\frac{(1-P)\mu^{\alpha}\left(\mathcal{S} - \mathcal{S}^1\right)^2}{\mathcal{S}\mathcal{S}^1} - \beta^{\alpha}\left(\mathcal{I} - \mathcal{I}^1\right)\left(\mathcal{S} - \mathcal{S}^1\right) \\
&- \mathcal{I}(\eta^{\alpha} + \mu^{\alpha})\left(1 - \frac{\beta^{\alpha}\mathcal{S}}{\eta^{\alpha} + \mu^{\alpha}}\right)
\end{aligned}$$

$\Rightarrow {}^{c}_{0}D^{\alpha}_{t}u(t) \leq 0$ for $R_c < 1$ and ${}^{c}_{0}D^{\alpha}_{t}u(t) = 0$ only if $\mathcal{S} = \mathcal{S}^1$, $\mathcal{I} = 0$ thus, E_d is globally asymptotically stable. □

Theorem 5. *For given $t > 0$ and $0 < \alpha \leq 1$, the model (1)-(3) is said to be globally asymptotically stable at endemic equilibrium $E_e = (\mathcal{S}^*, \mathcal{I}^*)$, which is contained in the region Γ if $R_v < 1$.*

Proof. Consider the Lyaponuv function $V : \Gamma \to R$ defined as

$$v = A_1\left(\mathcal{S} - \mathcal{S}^* - \mathcal{S}^* log\frac{\mathcal{S}}{\mathcal{S}^*}\right) + A_1\left(\mathcal{I} - \mathcal{I}^* - \mathcal{I}^* log\frac{\mathcal{I}}{\mathcal{I}^*}\right),$$

where $A_i, i = 1, 2$ are positive constants to be chosen later.

$$\begin{aligned}
{}^{c}_{0}D^{\alpha}_{t}v(t) &= A_1\left(1 - \frac{\mathcal{S}^*}{\mathcal{S}}\right) {}^{c}_{0}D^{\alpha}_{t}\mathcal{S}(t) + A_2\left(1 - \frac{\mathcal{I}^*}{\mathcal{I}}\right) {}^{c}_{0}D^{\alpha}_{t}\mathcal{I}(t) \\
&= A_1(\mathcal{S} - \mathcal{S}^*)\left(\frac{(1-P)\mu^{\alpha}}{\mathcal{S}} - \beta^{\alpha}\mathcal{I} - \mu^{\alpha}\right) + A_2(\mathcal{I} - \mathcal{I}^*)\left(\beta^{\alpha}\mathcal{S} - (\eta^{\alpha} - \mu^{\alpha})\right).
\end{aligned}$$

After some calculations, we get

$$\begin{aligned} {}_0^{\mathcal{C}}D_t^{\alpha} v(t) &= -\frac{A_1(1-P)\mu^{\alpha}\left(\mathcal{S}-\mathcal{S}^*\right)^2}{\mathcal{S}\mathcal{S}^*} - A_1\beta^{\alpha}\left(\mathcal{S}-\mathcal{S}^*\right)\left(\mathcal{I}-\mathcal{I}^*\right) \\ &+ A_2\beta^{\alpha}\left(\mathcal{S}-\mathcal{S}^*\right)\left(\mathcal{I}-\mathcal{I}^*\right) \\ &= -\frac{A_1(1-P)\mu^{\alpha}\left(\mathcal{S}-\mathcal{S}^*\right)^2}{\mathcal{S}\mathcal{S}^*} + \left(\mathcal{S}-\mathcal{S}^*\right)\left(\mathcal{I}-\mathcal{I}^*\right)\left(A_1-A_2\right). \end{aligned}$$

For $A_1 = A_2 = 1$, we have

$$ {}_0^{\mathcal{C}}D_t^{\alpha} v(t) = -\frac{A_1(1-P)\mu^{\alpha}\left(\mathcal{S}-\mathcal{S}^*\right)^2}{\mathcal{S}\mathcal{S}^*} \leq 0$$

$\Rightarrow {}_0^{\mathcal{C}}D_t^{\alpha} v(t) \leq 0$ for $R_v > 1$ and $\Rightarrow {}_0^{\mathcal{C}}D_t^{\alpha} v(t) = 0$ if $\mathcal{S} = \mathcal{S}^*$ then E_e is globally asymptotically stable. □

3. NONSTANDARD GRÜNWALD-LETNIKOV SCHEME

In this Section we derive a nonstandard Grünwald-Letnikov (NSGL) scheme to solve the system (1)-(3). Nonstandard finite difference techniques are the class of numerical schemes that retain the physical behavior of continuous systems, therefore are applied to compute the solution of various models [17–19]. We sssume that the time interval $(0,t)$ is divided into n uniform sub-intervals with the grid points $t_0 < t_1 < \cdots < t_{n+1} = t = (n+1)h$ where $h = t_{k+1} - t_k, k = 1 \cdots n$. The Grünwald-Letnikov approximation for the Caputo fractional derivative is given by

$$D_*^{\alpha} u(t_{n+1}) = \frac{1}{h^{\alpha}} \left(u(t_{n+1}) - \sum_{v=1}^{n+1} c_v^{\alpha} u(t_{n+1-v}) - r_{n+1}^{\alpha} u_0 \right), \tag{27}$$

where $u_0 = u(t_0), c_v^{\alpha} = (1 - \frac{\alpha+1}{v}) c_{v-1}^{\alpha}; c_1^{\alpha}$ and $r_{n+1}^{\alpha} = h^{\alpha} r_0^{\alpha}(t_{n+1}) = \frac{(n+1)^{-\alpha}}{\Gamma(1-\alpha)}$ [15]. Now the following result is helpful in proving other results in this article

Lemma 6. *[16] Let $0 < \alpha < 1$, then all the factors defined by $c_v^{\alpha} = (-1)^{v-1}\binom{\alpha}{v}$ are positive and also satisfy the relation $c_v^{\alpha} = O\left(\frac{1}{v^{v+\alpha}}\right)$ as $v \to \infty$. Moreover, we have the following expressions*
$0 \leq c_{v+1}^{\alpha} < c_v^{\alpha} < \cdots < c_1^{\alpha} = \alpha < 1$
and
$0 < a_{n+1}^{\alpha} < a_n^{\alpha} < \cdots < a_1^{\alpha} = \frac{1}{\Gamma(1-\alpha)} < 1$

It is obvious from the above Lemma that for $0 < \alpha < 1$, all coefficients c_v^{α} will always be positive and satisfy $0 < c_n^{\alpha} < c_{n-1}^{\alpha} < \cdots < c_1^{\alpha} = \alpha$ for $n \geq 1$. Furthermore, for $0 < \alpha < 1$ we have $\alpha + \frac{1}{\Gamma(1-\alpha)} > 1$. Also, $\sum_{v=1}^{\infty} c_v^{\alpha} = 1$. If the Grünwald-Letnikov approximation is applied to the left hand sides of the system (1)-(3) and right hand

sides of the system to approximate it non-locally, then we have

$$\begin{aligned}
\frac{1}{\Psi(h)^\alpha}\left(\mathcal{S}_{n+1}-\sum_{v=1}^{n+1}c_v^\alpha \mathcal{S}_{n+1-v}-a_{n+1}^\alpha \mathcal{S}_0\right) &= (1-P)\mu^\alpha-\beta^\alpha \mathcal{S}_{n+1}\mathcal{I}_n-\mu^\alpha \mathcal{S}_{n+1}\\
\frac{1}{\Psi(h)^\alpha}\left(\mathcal{I}_{n+1}-\sum_{v=1}^{n+1}c_v^\alpha I_{n+1-v}-a_{n+1}^\alpha \mathcal{I}_0\right) &= \beta^\alpha \mathcal{S}_n\mathcal{I}_n-(\mu^\alpha+\eta^\alpha)\mathcal{I}_{n+1}\\
\frac{1}{\Psi(h)^\alpha}\left(\mathcal{R}_{n+1}-\sum_{v=1}^{n+1}c_v^\alpha \mathcal{R}_{n+1-v}-a_{n+1}^\alpha \mathcal{R}_0\right) &= P\mu^\alpha+\eta^\alpha I_n-\mu^\alpha \mathcal{R}_{n+1}
\end{aligned}$$

and after simplification, we have

$$\mathcal{S}_{n+1} = \frac{\sum_{v=1}^{n+1}c_v^\alpha \mathcal{S}_{n+1-v}+a_{n+1}^\alpha \mathcal{S}_0+\Psi(h)^\alpha(1-P)\mu^\alpha}{1+\Psi(h)^\alpha\mu^\alpha+\Psi(h)^\alpha\beta^\alpha\mathcal{I}_n} \tag{28}$$

$$\mathcal{I}_{n+1} = \frac{\sum_{v=1}^{n+1}c_v^\alpha \mathcal{I}_{n+1-v}+a_{n+1}^\alpha \mathcal{I}_0+\Psi(h)^\alpha\beta^\alpha\mathcal{S}_n\mathcal{I}_n}{1+\Psi(h)^\alpha(\mu^\alpha+\eta^\alpha)} \tag{29}$$

$$\mathcal{R}_{n+1} = \frac{\sum_{v=1}^{n+1}c_v^\alpha \mathcal{R}_{n+1-v}+a_{n+1}^\alpha \mathcal{R}_0+\Psi(h)^\alpha P\mu^\alpha+\Psi(h)^\alpha\eta^\alpha\mathcal{I}_n}{1+\Psi(h)^\alpha\mu^\alpha} \tag{30}$$

3.1. POSITIVITY OF THE SOLUTION

It is evident that population of any species can never be negative so it is self explanatory that population is always non negative. In this article we will construct a scheme ensuring the positivity of the solution. The following Theorem ensures that the proposed technique is positivity preserving.

Theorem 7. *Assume that all the variables and control parameters involved in the model are non-negative, i.e.* $\mathcal{S}_0$*,* $\mathcal{I}_0$*, and* $\mathcal{R}_0$ *are greater than or equal to zero and* μ^α*,* β^α*,* η^α*,* P *and* $\Psi(h)^\alpha$ *are all strictly positive, then* $\mathcal{S}_n$*,* $\mathcal{I}_n$*, and* $\mathcal{R}_n$ *are non-negative.*

Proof. Considering equations (28)-(30), for $n=0$, we have

$$\mathcal{S}_1 = \frac{c_1^\alpha \mathcal{S}_0+a_1^\alpha \mathcal{S}_0+\Psi(h)^\alpha(1-P)\mu^\alpha}{1+\Psi(h)^\alpha\mu^\alpha+\Psi(h)^\alpha\beta^\alpha\mathcal{I}_0}$$

Noticing the restriction on the variables and the parameters, it is obvious that $\mathcal{S}_1>0$. In the same fashion, it is clear that $\mathcal{I}_1>0$ and $\mathcal{R}_1>0$. Next, we suppose that $\mathcal{S}_n>0$,

$\mathcal{I}_n > 0$ and $\mathcal{R}_n > 0$ $\forall n = 1, 2, \cdots, n-1$. Thus, for a positive n, we have

$$\begin{aligned}
\mathcal{S}_{n+1} &= \frac{\sum_{v=1}^{n+1} c_v^{\alpha} \mathcal{S}_{n+1-v} + a_{n+1}^{\alpha} \mathcal{S}_0 + \Psi(h)^{\alpha}(1-P)\mu^{\alpha}}{1 + \Psi(h)^{\alpha}\mu^{\alpha} + \Psi(h)^{\alpha}\beta^{\alpha}\mathcal{I}_n} \\
\mathcal{I}_{n+1} &= \frac{\sum_{v=1}^{n+1} c_v^{\alpha} \mathcal{I}_{n+1-v} + a_{n+1}^{\alpha} \mathcal{I}_0 + \Psi(h)^{\alpha}\beta^{\alpha}\mathcal{S}_n\mathcal{I}_n}{1 + \Psi(h)^{\alpha}(\mu^{\alpha} + \eta^{\alpha})} \\
\mathcal{R}_{n+1} &= \frac{\sum_{v=1}^{n+1} c_v^{\alpha} \mathcal{R}_{n+1-v} + a_{n+1}^{\alpha} \mathcal{R}_0 + \Psi(h)^{\alpha}P\mu^{\alpha} + \Psi(h)^{\alpha}\eta^{\alpha}\mathcal{I}_n}{1 + \Psi(h)^{\alpha}\mu^{\alpha}}
\end{aligned}$$

So, by using the principle of the mathematical induction and straightforward calculation, we conclude that $\mathcal{S}_{n+1} > 0$, $\mathcal{I}_{n+1} > 0$ and $\mathcal{R}_{n+1} > 0$. Hence the proof is complete. □

3.2. BOUNDEDNESS

In this Section, we will prove another important property of the population dynamics model. The following Theorem is helpful in this regard.

Theorem 8. *Suppose that* $\mathcal{S}_0 + \mathcal{I}_0 + \mathcal{R}_0 = 1$, $\beta^{\alpha} > 0, \eta^{\alpha} > 0, \mu^{\alpha} > 0$ *and* $\Psi(h)^{\alpha} > 0$ *for* $\alpha \in (0,1)$. *Then there is a constant* $\mathcal{N}(N_0+1,\alpha) = \frac{\left(\alpha + \frac{N_0+1}{\Gamma(1-\alpha)} + (\Psi(h)^{\alpha})\mu^{\alpha}\right)}{1+\Psi(h)^{\alpha}\mu^{\alpha}}$ *such that* $S_{n+1}, I_{n+1}, R_{n+1} < \mathcal{N}(N_0+1,\alpha)$ *for* $n = 0, 1, 2, ..., N_0$.

Proof.

$$\begin{aligned}
\mathcal{S}_{n+1} &= \frac{\Psi(h)^{\alpha}(1-P)\mu^{\alpha} + \sum_{v=1}^{n+1} c_v^{\alpha} \mathcal{S}_{n+1-v} + a_{n+1}^{\alpha} \mathcal{S}_0}{(1 + \Psi(h)^{\alpha}(\beta^{\alpha}\mathcal{I}_n + \mu^{\alpha}))} \\
\mathcal{I}_{n+1} &= \frac{\sum_{v=1}^{n+1} c_v^{\alpha} \mathcal{I}_{n+1-v} + a_{n+1}^{\alpha} \mathcal{I}_0 + \Psi(h)^{\alpha}\beta^{\alpha}\mathcal{S}_{n+1}\mathcal{I}_n}{(1 + \Psi(h)^{\alpha}(\eta^{\alpha} + \mu^{\alpha}))} \\
\mathcal{R}_{n+1} &= \frac{\sum_{v=1}^{n+1} c_v^{\alpha} \mathcal{R}_{n+1-v} + a_{n+1}^{\alpha} \mathcal{R}_0 + \Psi(h)^{\alpha}\eta^{\alpha}\mathcal{I}_{n+1} + P\mu^{\alpha}}{(1 + \Psi(h)^{\alpha}\mu^{\alpha})}
\end{aligned}$$

then, after adding all the above equations, we have

$$\mathcal{S}_{n+1} + \mathcal{I}_{n+1} + \mathcal{R}_{n+1} = \frac{\left(\sum_{v=1}^{n+1} c_v^{\alpha}(\mathcal{S}_{n+1-v} + \mathcal{I}_{n+1-v} + \mathcal{R}_{n+1-v}) + a_{n+1}^{\alpha} + \Psi(h)^{\alpha}\mu^{\alpha}\right)}{(1 + \Psi(h)^{\alpha}\mu^{\alpha})} \quad (31)$$

Using Lemma 6 and equation (31) for $n = 0$, we have the following expression

$$\begin{aligned}
\mathcal{S}_1 + \mathcal{I}_1 + \mathcal{R}_1 &= \frac{\sum_{v=1}^{1} c_v^{\alpha}(\mathcal{S}_{1-v} + \mathcal{I}_{1-v} + \mathcal{R}_{1-v}) + a_1^{\alpha} + \Psi(h)^{\alpha}\mu^{\alpha}}{1 + \Psi(h)^{\alpha}\mu^{\alpha}} \\
&= \frac{c_1^{\alpha}(\mathcal{S}_0 + \mathcal{I}_0 + \mathcal{R}_0) + a_1^{\alpha} + \Psi(h)^{\alpha}\mu^{\alpha}}{1 + \Psi(h)^{\alpha}\mu^{\alpha}} \\
&= \frac{c_1^{\alpha} + a_1^{\alpha} + \Psi(h)^{\alpha}\mu^{\alpha}}{1 + \Psi(h)^{\alpha}\mu^{\alpha}} \\
&< \frac{\alpha + a_1^{\alpha} + \Psi(h)^{\alpha}\mu^{\alpha}}{1 + \Psi(h)^{\alpha}\mu^{\alpha}} \\
&= \frac{\alpha + \frac{1}{\Gamma(1-\alpha)} + \Psi(h)^{\alpha}\mu^{\alpha}}{1 + \Psi(h)^{\alpha}\mu^{\alpha}} \\
\mathcal{S}_1 + \mathcal{I}_1 + \mathcal{R}_1 &< \mathcal{N}(1, \alpha),
\end{aligned}$$

for $0 < \alpha < 1$. Similarly, for $n = 1$, we obtain

$$\begin{aligned}
\mathcal{S}_2 + \mathcal{I}_2 + \mathcal{R}_2 &= \frac{\sum_{v=1}^{2} c_v^{\alpha}(\mathcal{S}_{2-v} + \mathcal{I}_{2-v} + \mathcal{R}_{2-v}) + a_2^{\alpha} + \Psi(h)^{\alpha}\mu^{\alpha}}{1 + \Psi(h)^{\alpha}\mu^{\alpha}} \\
&= \frac{c_1^{\alpha}(\mathcal{S}_1 + \mathcal{I}_1 + \mathcal{R}_1) + c_2^{\alpha}(\mathcal{S}_0 + \mathcal{I}_0 + \mathcal{R}_0) + a_2^{\alpha} + \Psi(h)^{\alpha}\mu^{\alpha}}{1 + \Psi(h)^{\alpha}\mu^{\alpha}} \\
&< \frac{c_1^{\alpha}\mathcal{N}(1, \alpha) + c_2^{\alpha} + a_1^{\alpha} + \Psi(h)^{\alpha}\mu^{\alpha}}{1 + \Psi(h)^{\alpha}\mu^{\alpha}} \\
&< \frac{(c_1^{\alpha} + c_2^{\alpha})\mathcal{N}(1, \alpha) + \frac{1}{\Gamma(1-\alpha)} + \Psi(h)^{\alpha}\mu^{\alpha}}{1 + \Psi(h)^{\alpha}\mu^{\alpha}} \\
&= \frac{\mathcal{N}(1, \alpha)\sum_{v=1}^{\infty} c_v^{\alpha} + \frac{1}{\Gamma(1-\alpha)} + \Psi(h)^{\alpha}\mu^{\alpha}}{1 + \Psi(h)^{\alpha}\mu^{\alpha}}
\end{aligned}$$

So,

$$\mathcal{S}_2 + \mathcal{I}_2 + \mathcal{R}_2 < \frac{N(1, \alpha) + \frac{1}{\Gamma(1-\alpha)} + \Psi(h)^{\alpha}\mu^{\alpha}}{1 + \Psi(h)^{\alpha}\mu^{\alpha}} = \mathcal{N}(2, \alpha)$$

$\Rightarrow \mathcal{S}_2+\mathcal{I}_2+\mathcal{R}_2<\mathcal{N}(2,\alpha)$, which is for $0<\alpha<1$. Similar result is obtained for $n=2$

$$\begin{aligned}\mathcal{S}_3+\mathcal{I}_3+\mathcal{R}_3 &= \frac{\sum_{v=1}^{3}c_v^{\alpha}(\mathcal{S}_{n+1-v}+\mathcal{I}_{n+1-v}+\mathcal{R}_{n+1-v})+a_3^{\alpha}+\Psi(h)^{\alpha}\mu^{\alpha}}{1+\Psi(h)^{\alpha}\mu^{\alpha}}\\ &< \frac{c_1^{\alpha}\mathcal{N}(2,\alpha)+c_2^{\alpha}(\mathcal{N}_1,\alpha)+c_3^{\alpha}+a_3^{\alpha}+\Psi(h)^{\alpha}\mu^{\alpha}}{1+\Psi(h)^{\alpha}\mu^{\alpha}}\\ &< \frac{c_1^{\alpha}\mathcal{N}(2,\alpha)+c_2^{\alpha}(\mathcal{N}_2,\alpha)+c_3(\mathcal{N}_2,\alpha)+a_3^{\alpha}+\Psi(h)^{\alpha}\mu^{\alpha}}{1+\Psi(h)^{\alpha}\mu^{\alpha}}\\ &< \frac{\sum_{v=1}^{\infty}c_v^{\alpha}\mathcal{N}(2,\alpha)+a_1^{\alpha}+\Psi(h)^{\alpha}\mu^{\alpha}}{1+\Psi(h)^{\alpha}\mu^{\alpha}}\end{aligned}$$

So,

$$\mathcal{S}_3+\mathcal{I}_3+\mathcal{R}_3<\frac{\mathcal{N}(2,\alpha)+\frac{1}{\Gamma(1-\alpha)}+\Psi(h)^{\alpha}\mu^{\alpha}}{1+\Psi(h)^{\alpha}\mu^{\alpha}}=\mathcal{N}(3,\alpha) \tag{32}$$

$\Rightarrow \mathcal{S}_3+\mathcal{I}_3+\mathcal{R}_3<\mathcal{N}(3,\alpha)$, for $0<\alpha<1$.

Now, we suppose that for $n=3,4,.....N_0-1$, the following expression is satisfied,

$$\mathcal{S}_{n+1}+\mathcal{I}_{n+1}+\mathcal{R}_{n+1}<\frac{\mathcal{N}(N_0-1,\alpha)+\frac{1}{\Gamma(1-\alpha)}+\Psi(h)^{\alpha}\mu^{\alpha}}{1+\Psi(h)^{\alpha}\mu^{\alpha}} \tag{33}$$

Finally, for $0<\alpha<1$ and for $n=N_0$ we obtain that

$$\mathcal{S}_{N_0+1}+\mathcal{I}_{N_0+1}+\mathcal{R}_{N_0+1}<\frac{\mathcal{N}(N_0,\alpha)+\frac{1}{\Gamma(1-\alpha)}+\Psi(h)^{\alpha}\mu^{\alpha}}{1+\Psi(h)^{\alpha}\mu^{\alpha}}$$

This implies that $\mathcal{S}_{N_0+1}+\mathcal{I}_{N_0+1}+\mathcal{R}_{N_0+1}<\mathcal{N}(N_0+1,\alpha)$, where $0<\alpha<1$. Hence, by the principle of mathematical induction it is verified that for all $n\in\{0,.....N_0\}$, $\mathcal{S}_{n+1}+\mathcal{I}_{n+1}+\mathcal{R}_{n+1}<\mathcal{N}(N_0+1,\alpha)$. □

4. NUMERICAL SIMULATIONS

This Section is devoted for the presentation of numerical simulations with the help of proposed NSGL numerical scheme by choosing various values of parameters and fractional order α. First we demonstrate the graphical behavior of the model under study at DFE with the help of proposed numerical scheme.

In Figs. 1-3, we consider the values of the parameters as $\mu=0.4$, $\eta=0.3$, $\beta=0.8$, and $P=0.55$ so that the reproductive number is less than one. Now, all the graphs in Fig. 1 demonstrate the different trajectories followed by $\mathcal{S}(t)$, against each

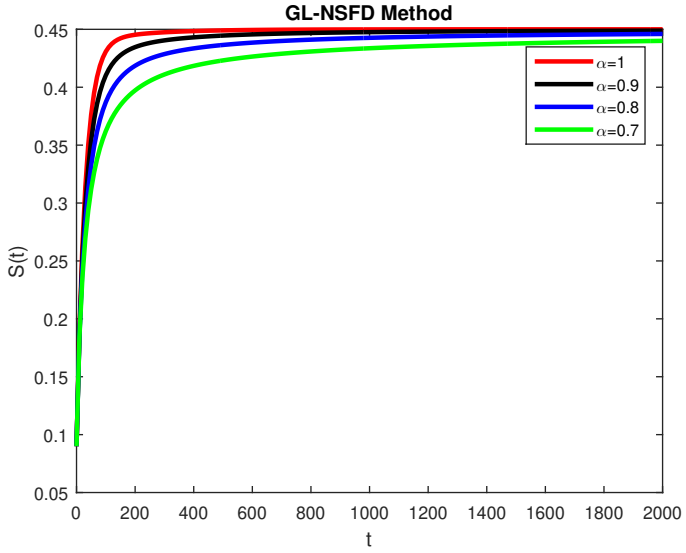

Fig. 1 – Solution behavior of susceptible population $\mathcal{S}(t)$ for various values of α with time step size $h = 10$ at disease free equilibrium.

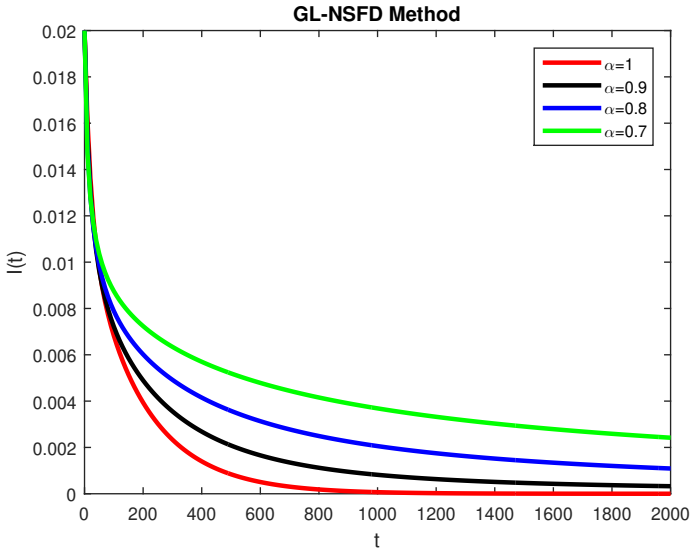

Fig. 2 – Solution behavior of infected population $\mathcal{I}(t)$ for various values of α with time step size $h = 10$ at disease free equilibrium.

α, for the convergence towards the equilibrium point. It is observed that for some greater value of α, the graph of $\mathcal{S}(t)$ is more steeper, as compared to the smaller val-

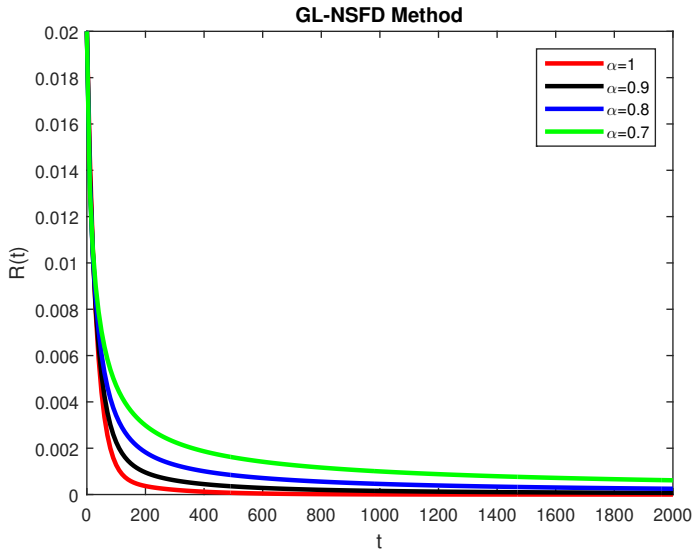

Fig. 3 – Solution behavior of recovered population $\mathcal{R}(t)$ for various values of α with time step size $h = 10$ at disease free equilibrium.

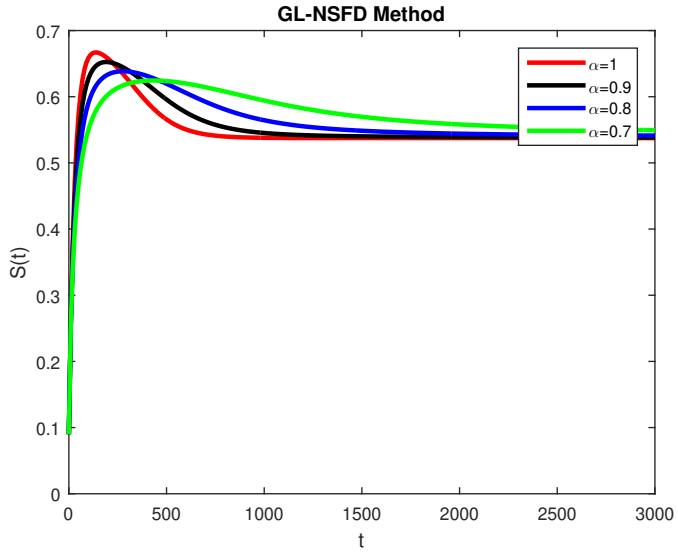

Fig. 4 – Solution behavior of susceptible population $\mathcal{S}(t)$ for various values of α with time step size $h = 10$ at endemic equilibrium.

ues of α. The graphs show that for the susceptible population it takes more time to reach the equilibrium point, when α is chosen smaller, for instance $\alpha = 0.7$. Equiva-

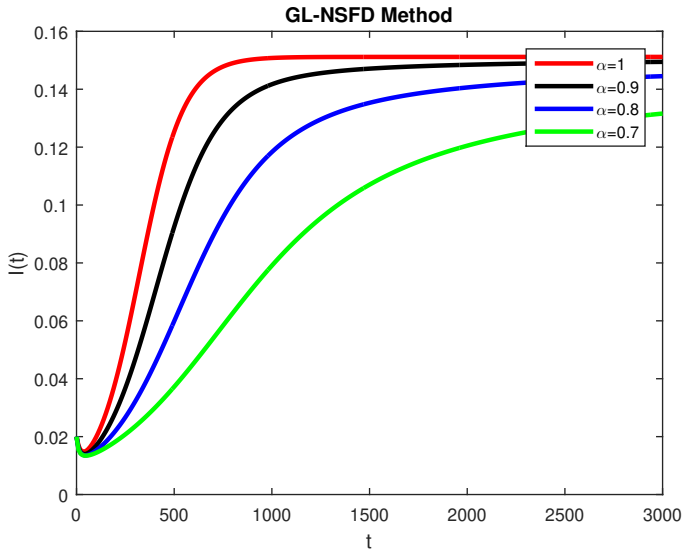

Fig. 5 – Solution behavior of infected population $\mathcal{I}(t)$ for various values of α with time step size $h = 10$ at endemic equilibrium.

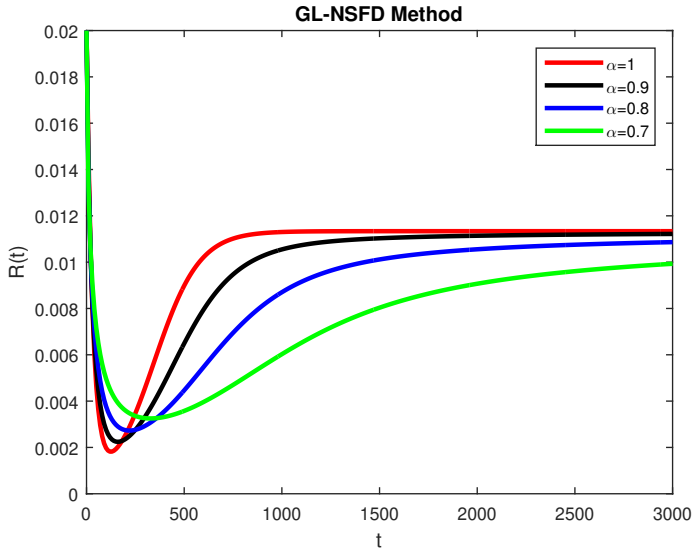

Fig. 6 – Solution behavior of recovered population $\mathcal{R}(t)$ for various values of α with time step size $h = 10$ at endemic equilibrium.

lently, graph grows slowly for smaller values of the fractional order parameter α. All the four graphs in Fig. 2 reflect the behavior of infected population with the passage

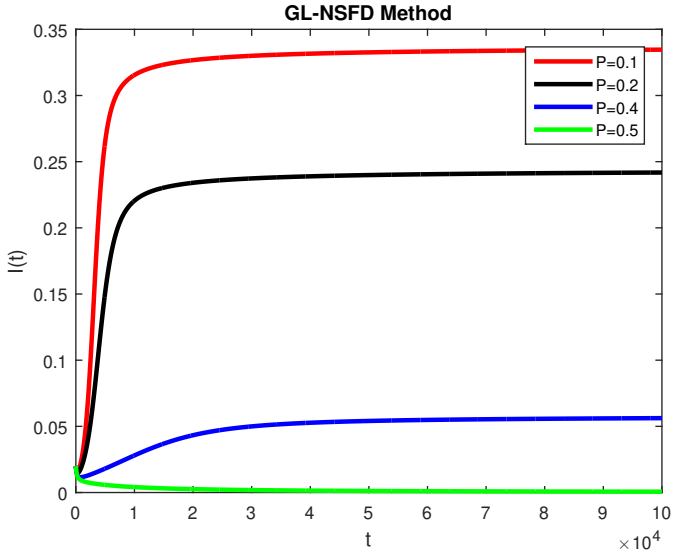

Fig. 7 – Solution behavior of infected population $\mathcal{I}(t)$ for various values of vaccination parameter P with time step size $h = 100$.

of time, selecting the time step size $h = 10$. All the graphs, for some different values of α, as highlighted in Figs. 2 and 3, converge towards the disease free steady state. As the time grows, the infected individuals are greater for the greater values of α as compared to the smaller values of α. But the trajectory converges fastly when α is greater and close to 1.

In Figs. 4-6, we consider the values of parameters as $\mu = 0.4$, $\eta = 0.3$, $\beta = 0.8$, and $P = 0.3$ so that the reproductive number is greater than one. The plots in Figs. 4-6 express the behavior of the state variables at EE. All the curves shown in the figures demonstrate the graphical path followed the state variables $\mathcal{S}(t)$, $\mathcal{I}(t)$, and $\mathcal{R}(t)$ for the various values of α. It is observed that all the graphical curves converge to the true endemic steady state.

Figure 7 demonstrates the effect of vaccination parameter P on infected population. It is observed that the increase in vaccination reduces the infection. It can be seen that all the graphical solution validate the positivity and boundedness of the proposed technique. Also, numerical simulations show that the designed techniques retains the stability of equilibria.

5. CONCLUSION

In this study, we have considered an extended fractional order SIR epidemic model with constant vaccination strategy and we have investigated its numerical so-

lution. The role of vaccination reproductive number in describing the disease communication and stability has been investigated. We have proposed an efficient explicit numerical technique that sustains the positivity and boundedness of the continuous model. The positivity and boundedness of the numerical technique is mathematically proved and verified by the numerical simulations. Graphically, the disease dynamics has been described with the help of vaccination strategy.

REFERENCES

1. M. Suhrcke *et al.*, *The Impact of Economic Crises on Communicable Disease Transmission and Control: A Systematic Review of the Evidence*, PLoS ONE **6**, e20724 (2011).
2. O. D. Makinde, *Adomian decomposition approach to a SIR epidemic model with constant vaccination strategy*, Applied Mathematics and Computation **184**, 842-848 (2007).
3. A. Mhlanga, *Dynamical analysis and control strategies in modelling Ebola virus disease*, Adv. Differ. Equ. **2019**, 458 (2019).
4. Z. E. Rhoubari, H. Besbassi, K. Hattaf, and N. Yousfi, *Mathematical Modeling of Ebola Virus Disease in Bat Population*, Discrete Dynamics in Nature and Society, 5104524 (2018).
5. I. Kurane and T. Takasaki, *Dengue fever and dengue haemorrhagic fever: challenges of controlling an enemy still at large*, Reviews in Medical Virology **11**, 301–311 (2015).
6. G. Rossi *et al.*, *The Potential Role of Direct and Indirect Contacts on Infection Spread in Dairy Farm Networks*, PLoS Comput. Biol. **13**, e1005301 (2017).
7. N. Sene, *SIR epidemic model with Mittag-Leffler fractional derivative*, Chaos, Solitons and Fractals **137**, 109833 (2020).
8. F. A. Rihan, Q. M. Al-Mdallal, J. AlSakaji, and A. Hashish, *A fractional-order epidemic model with time-delay and nonlinear incidence rate*, Chaos, Solitons and Fractals **126**, 97–105 (2019).
9. S. Ullah, M. A. Khan, and M. Farooq, *A fractional model for the dynamics of TB virus*, Chaos, Solitons and Fractals **116**, 63–71 (2018).
10. M. Shen, Z. Peng, Y. Xiao, and L. Zhang, *Modelling the epidemic trend of the 2019 novel coronavirus outbreak in China*, bioRxiv (2020).
11. M. Saeedian, M. Khalighi, N. A. Tafreshi, G. R. Jafari, and M. Ausloos, *Memory effects on epidemic evolution: The susceptible-infected-recovered epidemic model*, Phys. Rev. E **95**, 022409 (2017).
12. S. Ucar, E. Ucar, N. Ozdemir, and Z. Hammouch, *Mathematical analysis and numerical simulation for a smoking model with Atangana-Baleanu derivative*, Chaos, Solitons and Fractals **118**, 300–306 (2019).
13. M. A. Khan and A. Atangana, *Modeling the dynamics of novel coronavirus (219-nCov) with fractional derivative*, Alexandria Engineering Journal **59**, 2379–2389 (2020).
14. A. Mouaouine, A. Boukhouima, K. Hattaf, and N. Yousfi, *A fractional order SIR epidemic model with nonlinear incidence rate*, Adv. Differ. Equ. **2018**, 160 (2018).
15. R. Scherer, S. L. Kalla, Y. Tang, and J. Huang, *The Grünwald-Letnikov method for fractional differential equations*, Computers and Mathematics with Applications **62**, 902–917 (2011).
16. A. J. Arenas, G. González-Parra, and B. M. Chen-Charpentier, *Construction of nonstandard finite difference schemes for the SI and SIR epidemic models of fractional order*, Mathematics and Computers in Simulation **121**, 48-63 (2016).
17. Z. Iqbal, N. Ahmed, D. Baleanu, W. Adel, M. Rafiq, M. A. Rehman, and A. S. Alshomrani,

Positivity and boundedness preserving numerical algorithm for the solution of fractional nonlinear epidemic model of HIV/AIDS transmission, Chaos, Solitons and Fractals **134**, 109706 (2020).

18. Z. Iqbal, N. Ahmed, D. Baleanu, M. Rafiq, M. S. Iqbal, and M. A. Rehman, *Structure preserving computational technique for fractional-order Schnakenberg model*, Computational and Applied Mathematics **39**, 61 (2020).
19. J. Calatayud and M. Jornet, *Stochastic simulation of epidemics using the maximum entropy principle and generalized polynomial chaos expansions*, Rom. Rep. Phys. **72**, 112 (2020).
20. S. V. Ershkov, V. Christianto, A. Rachinskaya, and E. Y. Prosviryakov, *A nonlinear heuristic model for estimation of Covid-19 impact to world population*, Rom. Rep. Phys. **72**, 605 (2020).
21. M. Alquran, I. Jaradat, D. Baleanu, and M. Syam, *The Duffing model endowed with fractional time derivative and multiple pantograph time delays*, Rom. J. Phys. **64**, 107 (2019).
22. P. Li *et al.*, *PT-symmetric optical modes and spontaneous symmetry breaking in the space-fractional Schrödinger equation*, Rom. Rep. Phys. **71**, 106 (2019).
23. I. Abu Irwaq, M. Alquran, I. Jaradat, M. S. M. Noorani, S. Momani, and D. Baleanu, *Numerical investigations on the physical dynamics of the coupled fractional Boussinesq-Burgers system*, Rom. J. Phys. **65**, 111 (2020).
24. P. Li *et al.*, *Vortex solitons in fractional nonlinear Schrödinger equation with the cubic-quintic nonlinearity*, Chaos, Solitons and Fractals **137**, 109783 (2020).
25. Y. Qiu *et al.*, *Stabilization of single- and multi-peak solitons in the fractional nonlinear Schrödinger equation with a trapping potential*, Chaos, Solitons and Fractals **140**, 110222 (2020).
26. P. Li *et al.*, *Symmetry breaking of spatial Kerr solitons in fractional dimension*, Chaos, Solitons and Fractals **132**, 109602 (2020).
27. Y. Qiu *et al.*, *Soliton dynamics in a fractional complex Ginzburg-Landau model*, Chaos, Solitons and Fractals **131**, 109471 (2020).
28. A. Izadkhah, K. Nouri, and A. Nikoobin, *Proportional integral derivative control of fractional-order for a quarter-vehicle active suspension system*, Rom. J. Phys. **65**, 103 (2020).
29. N. Ahmed, D. Baleanu, A. Korkmaz, M. Rafiq, M. A. Rehman, and M. Ali, *Positivity preserving computational techniques for nonlinear autocatalytic chemical reaction model*, Rom. Rep. Phys. **72**, 121 (2020).
30. M. Ali *et al.*, *Dynamics of integer-fractional time-derivative for the new two-mode Kuramoto-Sivashinsky model*, Rom. Rep. Phys. **72**, 103 (2020).
31. M. A. Abdelkawy, *An improved collocation technique for distributed-order fractional partial differential equations*, Rom. Rep. Phys. **72**, 104 (2020).
32. M. Alquran *et al.*, *Chaotic and solitonic solutions for a new time-fractional two-mode Korteweg-de Vries equation*, Rom. Rep. Phys. **72**, 117 (2020).
33. P. Li *et al.*, *Metastable soliton necklaces supported by fractional diffraction and competing nonlinearities*, Opt. Express **28**, 34472–34488 (2020).